WATER RESOURCES RESEARCH, VOL. 49, 3618–3625, doi:10.1002/wrcr.20209, 2013

Engineered injection and extraction to enhance reaction for improved in situ remediation

Amy N. Piscopo,[1] Roseanna M. Neupauer,[1] and David C. Mays[2]

Received 28 June 2012; revised 10 March 2013; accepted 20 March 2013; published 21 June 2013.

[1] During in situ remediation, a treatment solution is often injected into a contaminated aquifer to degrade the groundwater contaminant. Since contaminant degradation reactions occur only at locations where the treatment solution and groundwater contaminant overlap, mixing of the treatment solution and the contaminated groundwater is necessary for reaction to occur. Mixing results from molecular diffusion and pore-scale dispersion, which operate over small length scales; thus, mixing during in situ remediation can only occur where the separation distance between the treatment solution and contaminated groundwater is small. To promote mixing, advection can be used to spread the treatment solution into the contaminated groundwater to increase the extent of the region where the two solutions coexist. A certain degree of passive spreading is the natural consequence of aquifer heterogeneity, which is manifested as macrodispersion. An alternative mechanism is active spreading, in which unsteady flows lead to stretching and folding of plumes. Active spreading can be accomplished by engineered injection and extraction (EIE), in which clean water is injected and extracted at wells surrounding a contaminant plume to create unsteady flow fields that stretch and fold the treatment solution and contaminant plumes. For a model system in which nested plumes of two reactants undergo scalar transport and instantaneous reaction, the simulation results reported here indicate that EIE enhances degradation of groundwater contamination in homogeneous and heterogeneous aquifers compared to baseline models without EIE. Furthermore, this study shows that the amount of reaction provided by the spreading due to EIE is greater than the amount of reaction due to spreading from heterogeneity alone.

Citation: Piscopo, A. N., R. M. Neupauer, and D. C. Mays (2013), Engineered injection and extraction to enhance reaction for improved in situ remediation, *Water Resour. Res.*, *49*, 3618–3625, doi:10.1002/wrcr.20209.

1. Introduction

[2] Energy-efficient methods of remediating contaminated groundwater, such as in situ remediation, have become increasingly relevant given the current state of rising water and energy usage across the globe. In situ remediation, where a treatment solution (containing oxidants, electron donors, or nutrients) is injected into the aquifer, is a commonly used method for treating contaminated groundwater. For example, chemical oxidants, like potassium permanganate, can be used to treat chlorinated solvents, like trichloroethylene [*Yan and Schwartz*, 1999], a common groundwater contaminant associated with industrial degreasing [*Wartenburg et al.*, 2000]. Contaminant degradation requires mixing the treatment solution and the contaminated groundwater [*MacDonald and Kitanidis*, 1993; *Dentz et al.*, 2011], but accomplishing mixing in aquifers is challenging since the laminar flows characteristic of porous media preclude the turbulent eddies that promote mixing in open channel flows or engineered reactors. Accordingly, considerable work has been undertaken to model and quantify plume spreading and mixing in the context of groundwater remediation. Here the term *spreading* indicates plume reconfiguration by advection and macrodispersion without dilution, and the term *mixing* indicates molecular diffusion and pore-scale dispersion with dilution [*Dentz et al.*, 2011]. Spreading by advection and macrodispersion can increase the contact area between the treatment solution and contaminant, which thereby promotes mixing of these reactants since molecular diffusion and pore-scale dispersion only operate over small characteristic length scales [*Weeks and Sposito*, 1998; *Bellin et al.*, 2011].

[3] Because spreading is a strictly advective process, it can be interpreted as the consequence of spatially varying velocity [*Le Borgne et al.*, 2010]. In aquifers, spatially varying velocity generally results from heterogeneity of hydraulic conductivity [*Dagan*, 1989, §4.3.5; *Kitanidis*, 1994]. Because heterogeneous aquifers are the rule rather than the exception, essentially any in situ remediation scheme will

[1]Department of Civil, Environmental, and Architectural Engineering, University of Colorado Boulder, Boulder, Colorado, USA.
[2]Department of Civil Engineering, University of Colorado Denver, Denver, Colorado, USA.

Corresponding author: A. N. Piscopo, Department of Civil, Environmental, and Architectural Engineering, University of Colorado Boulder, ECOT 441, UCB 428, Boulder, CO 80309-0428, USA. (amy.piscopo@colorado.edu)

0043-1397/13/10.1002/wrcr.20209

therefore experience a certain degree of plume spreading. Plume spreading, in turn, increases the spatial extent of the plume interface, which is characterized by large contaminant concentration gradients. These large concentration gradients promote transverse dispersion, which increases mixing [*Cirpka*, 2005; *Rolle et al*., 2009], and increased mixing allows for increased contaminant degradation [*Castro-Alcala et al*., 2012]. However, in the current practice of in situ remediation, tactics to spread plumes of treatment solution into contaminated aquifers are limited: Either the treatment solution is left to travel with the ambient groundwater flow, or it is drawn through the aquifer using a downgradient pumping well [*U.S. Environmental Protection Agency*, 1998]. In either case, spreading is passive, in the sense that it results from naturally occurring velocity variations. In contrast, active spreading can be accomplished by deliberately imposing unsteady flows in the contaminated region of the aquifer. Active spreading is beneficial because it opens the possibility of improved plume spreading based on chaotic advection.

[4] Chaotic advection refers to a class of deterministic laminar flows in which the trajectories of fluid particles exhibit sensitive dependence on initial conditions [*Aref*, 1984; *Ottino*, 1989]. In such flows, fluid particles that are initially separated by a small distance will eventually be separated by a large distance (at least in certain regions of the flow field), which provides good spreading. In two-dimensional flows, chaotic advection generally results from active control that establishes unsteady flow using rotating rods [*Aref*, 1984], eccentric cylinders [*Swanson and Ottino*, 1990], or, particularly relevant to groundwater remediation, injection and extraction of fluid through wells. Recognizing its potential in groundwater remediation, *Sposito* [2006], *Bagtzoglou and Oates* [2007], and *Trefry et al*. [2012] have presented arguments for applying chaotic advection to groundwater remediation.

[5] A unifying theme in the spreading literature is the important role of stretching and folding. *Ottino* [1989] includes stretching and folding in his definition of fluid mixing as the "...efficient stretching and folding of material lines and surfaces." *Weeks and Sposito* [1998] emphasized the importance of stretching and folding for spreading plumes in groundwater. Folding is especially important because it allows stretching to continue even within a bounded domain [*Aref*, 2002], which is beneficial in the context of in situ remediation, where it is necessary to contain the contaminant within a limited area of the aquifer.

[6] *Mays and Neupauer* [2012] proposed a strategy to enhance plume spreading in groundwater, called engineered injection and extraction (EIE), in which a sequence of injections and extractions of clean water at an array of wells creates unsteady flow fields that stretch and fold the interface between the treatment solution and contaminated groundwater. They found that EIE can stretch and fold the interface, leading to enhanced spreading in aquifers. At least for the case of a homogeneous aquifer, they also demonstrated the presence of chaotic advection during EIE, which therefore places EIE in the class of flows known to optimize spreading under laminar conditions [*Ottino et al*., 1994].

[7] The goal of this paper is to demonstrate that EIE leads to enhanced reaction during in situ remediation, as compared to passive in situ remediation. In contrast to *Mays and Neupauer* [2012], who considered only advective transport during EIE, we consider advection, dispersion, and reaction. We show through numerical simulations that EIE can significantly enhance reaction during in situ remediation, relative to passive in situ remediation without EIE, for both homogeneous and heterogeneous model aquifers.

[8] The paper is structured as follows. In section 2, we describe the EIE system, and the approach taken for modeling transport and reaction. We consider only instantaneous reactions between the treatment solution and contaminant, which are both assumed to be aqueous and nonsorbing. In section 3, we present simulation results showing that EIE leads to enhanced reaction in homogeneous and heterogeneous model aquifers. In section 4, we discuss practical considerations of EIE and the limitations of our investigation.

2. Engineered Injection and Extraction System

[9] The model analyzed in this study represents a confined, two-dimensional, isotropic aquifer with ambient groundwater flow traveling from east to west at a rate of 0.02 m/d. A circular plume of treatment solution with radius 6.25 m is located at the center of a circular plume of contaminated groundwater with outer radius 12.5 m, centered at the origin as shown in Figure 1. Four wells are placed symmetrically around the plume, each at a distance of $L = 25$ m from the origin.

[10] During EIE, wells are operated in a sequence at preset rates of injection or extraction of clean water. This study uses the 12-step sequence shown in Table 1, which is the same sequence used by *Mays and Neupauer* [2012]. Each step of the sequence lasts for $\Delta t = 6.25$ days, and only one well operates during any given step. The sequence is designed such that no net injection or extraction of water occurs. This particular EIE sequence is only one example that could be used to achieve stretching and folding under the imposed constraints. It was chosen because it creates

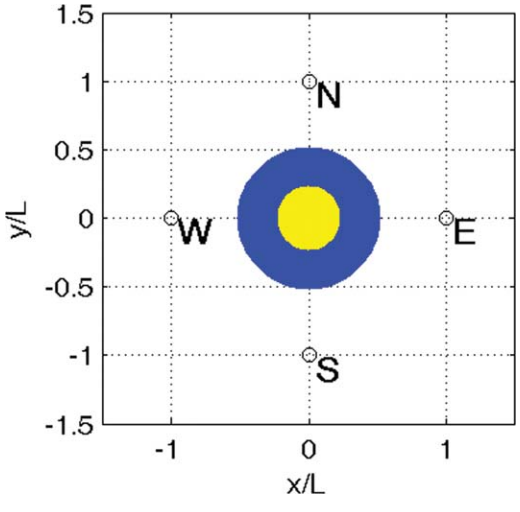

Figure 1. Plan view of model aquifer showing the initial positions of the treatment solution (yellow) and contaminant (blue) particles. Particles are placed on a regular grid with $0.01L$ (0.25 m) spacing. The small open circles denote the four wells, identified by cardinal direction.

Table 1. Engineered Injection and Extraction Sequence Used in This Study[a]

Step	1	2	3	4	5	6	7	8	9	10	11	12
Active Well	W	E	W	E	W	E	S	N	S	N	S	N
Injection Rate (m^3/d)	875	875	−250	−750	−400	−350	875	875	−250	−750	−400	−350
$\pi\Lambda^2$	3.5	3.5	−1.0	−3.0	−1.6	−1.4	3.5	3.5	−1.0	−3.0	−1.6	−1.4

[a]Negative injection rates represent extraction.

stretching and folding, while avoiding extraction of treatment solution at the active extraction wells. This allows the treatment solution to remain in the aquifer where it can react with the contaminant, thereby avoiding reaction in the wells where it could lead to clogging [*Bagtzoglou and Oates*, 2007; *Li et al*., 2010; *MacDonald et al*., 1999].

[11] Transport of the treatment solution and contaminant in the model aquifer is described by the advection-dispersion reaction equation, given by

$$\frac{\partial C_j}{\partial t} = -\nabla \cdot (\mathbf{v}C_j) + \nabla \cdot \mathbf{D}\nabla C_j - R. \tag{1}$$

where C_j is the concentration of the jth species ($j = 1$ for the treatment solution, $j = 2$ for contaminant, and $j = 3$ for the reaction product), t is time, R is the reaction rate, $\mathbf{v}=(v_x,v_y)$ is the groundwater velocity vector, and $\mathbf{D}$ is the dispersion tensor, with components given by

$$\begin{aligned} D_{xx} &= \alpha_L \frac{{v_x}^2}{|\mathbf{v}|} + \alpha_{TH} \frac{{v_y}^2}{|\mathbf{v}|}, \\ D_{xy} &= D_{yx} = (\alpha_L - \alpha_{TH}) \frac{v_x v_y}{|\mathbf{v}|}, \\ D_{yy} &= \alpha_L \frac{{v_y}^2}{|\mathbf{v}|} + \alpha_{TH} \frac{{v_x}^2}{|\mathbf{v}|}, \end{aligned} \tag{2}$$

[12] where α_L and α_{TH} are longitudinal and transverse dispersivities. The velocity in (1) and (2) are calculated from Darcy's law

$$\mathbf{v} = -\frac{1}{n}\mathbf{K}\nabla h, \tag{3}$$

Table 2. Parameter Values Used in Modeling Flow Fields, Dispersion, and Reaction

Parameter	Value
Specific storage, S_s	0.000001 m
Mean hydraulic conductivity, K	0.5 m/d
Ambient groundwater velocity	0.02 m/d
Aquifer thickness, b	10 m
Aquifer domain length	300.25 m
Finite difference grid discretization	0.25 m
Well spacing, L	25 m
Number of treatment solution particles	1961
Number of contaminant particles	5896
Hydraulic gradient	0.01
Variance of ln K	0.50
Variogram type	Spherical
Correlation length, λ, of ln K	6.25 m
Longitudinal dispersivity, α_L	0.05 m
Transverse dispersivity, α_{TH}	0.005 m
Duration of injection or extraction step, Δt	6.25 d
Porosity	0.25
Initial mass per treatment solution particle	4 mg
Initial mass per contaminant particle	1 mg

where n is porosity, $\mathbf{K}$ is the hydraulic conductivity tensor, and h is hydraulic head which is obtained from the solution to the groundwater flow equation in a two-dimensional confined aquifer, given by

$$S_s \frac{\partial h}{\partial t} = \nabla \cdot \mathbf{K}\nabla h + Q_i \delta(x - x_{w_i})\delta(y - y_{w_i}), \tag{4}$$

where S_s is the specific storage, Q_i is the rate of injection during the ith step of the injection and extraction sequence,(x_{w_i}, y_{w_i}) are the coordinates of the active well during the ith step, and $\delta(.)$ is the Dirac delta function. We use MODFLOW [*Harbaugh et al*., 2000] to solve (4) using parameter values found in Table 2.

[13] Reaction is modeled as an instantaneous irreversible reaction given by

$$C_1 + C_2 \rightarrow C_3, \tag{5}$$

where reactants C_1 and C_2 are the concentrations of the treatment solution and groundwater contaminant, respectively, and C_3 is the concentration of the reaction product, which is assumed to be inert. An instantaneous reaction allows us to evaluate how reaction is enhanced by stretching and folding, not by chemical kinetics. For convenience, the 1:1 stoichiometric ratio in (5) is assumed to imply a 1:1 mass ratio as well.

[14] The contaminated groundwater and treatment solution are simulated as a collection of particles initially spaced $0.01L$ (0.25 m) apart on a regular grid. The particles are subject to advection, dispersion, and reaction as shown in (1)–(5). The advection and dispersion steps are modeled using a random walk process based on the Kolmogorov equation (6), given by [e.g., *Uffink*, 1989]

$$\frac{\partial C}{\partial t} = -\alpha_i \frac{\partial C}{\partial x_i} + \beta_{ij} \frac{\partial^2 C}{\partial x_i \partial x_j}, \tag{6}$$

where subscripts imply summation over repeated indices $i,j = \{x,y\}$, and α and β are drift and noise tensors, respectively, given by

$$\alpha_i = \lim_{\Delta t \to 0} \frac{1}{\Delta t} \langle \overline{S_i} \rangle, \tag{7}$$

$$\beta_{ij} = \lim_{\Delta t \to 0} \frac{1}{2\Delta t} \langle \overline{S_i S_j} \rangle, \tag{8}$$

where $\overline{S_i}$ is the step taken by the particle in a time interval Δt, and brackets denote statistical averaging. We rewrite

(1) to have the same form as the Kolmogorov equation to obtain

$$\frac{\partial C}{\partial t} = -\left(v_x - \frac{\partial D_{xx}}{\partial x} - \frac{\partial D_{yx}}{\partial y}\right)\frac{\partial C}{\partial x} - \left(v_y - \frac{\partial D_{xy}}{\partial x} - \frac{\partial D_{yy}}{\partial y}\right)\frac{\partial C}{\partial y} + D_{xx}\frac{\partial^2 C}{\partial x^2} + D_{xy}\frac{\partial^2 C}{\partial x \partial y} + D_{yx}\frac{\partial^2 C}{\partial x \partial y} + D_{yy}\frac{\partial^2 C}{\partial y^2} - R. \tag{9}$$

[15] The drift component of (9) is modeled in two steps: The advection portion (e.g., v_x) is handled by translating particles with MODPATH [*Pollock*, 1994], based on the flow fields obtained by solving (4) using MODFLOW [*Harbaugh et al*., 2000]. The particle displacements due to the derivatives of the dispersion coefficients are superimposed. Parameter values used in the model are summarized in Table 2.

[16] Note that the relationship between key aquifer parameters can be described by the dimensionless number Λ^2, given by

$$\Lambda^2 = \frac{Q\Delta t}{\pi n b L^2}, \tag{10}$$

where b is the aquifer thickness. Equivalent results would be obtained for any set of parameters that produce the sequence of Λ^2 shown in Table 1.

[17] In this study, we evaluate both homogeneous and heterogeneous aquifers. To model heterogeneity, a random field of ln K was generated using sequential Gaussian simulation in GSLIB [*Deutsch and Journel*, 1992]. The random ln K field is shown in Figure 2, and the statistical properties are shown in Table 2.

[18] The dispersion component of (1) is modeled by adding random displacements to the particle positions prior to the advection step. Random displacements in the direction of the local velocity vector and in the direction perpendicular to the local velocity vector are normally distributed with zero mean and variances of $2\alpha_L|\mathbf{v}|\Delta t$ and $2\alpha_{TH}|\mathbf{v}|\Delta t$, respectively, where Δt is the duration of the injection or extraction step. The longitudinal dispersivity α_L was selected to be approximately one tenth of the travel distance of the ambient groundwater during Δt. The remaining parameter values used to model dispersion are summarized in Table 2.

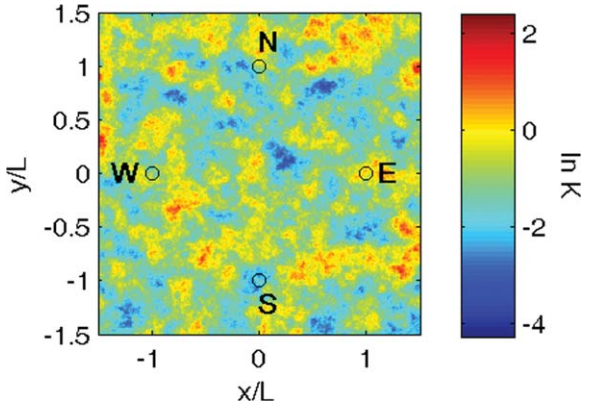

Figure 2. Random ln K field. Well locations are depicted with open circles and identified by cardinal direction.

[19] After each advection step, reaction is modeled by binning the treatment solution and contaminant particles into $0.025L$ by $0.025L$ (0.625 m × 0.625 m) bins. To simulate instantaneous and complete reaction with a 1:1 mass ratio between the treatment solution and contaminant, the entire mass of the limiting reactant within each bin is removed, and the mass of the excess reactant is reduced by its mass reacted. The remaining mass of the excess reactant is divided evenly among the particles of the excess reactant in the bin. All reacted mass is converted to reactant product such that mass is conserved.

3. Results

3.1. Reaction with Engineered Injection and Extraction

[20] Figure 3 illustrates the positions of treatment solution, groundwater contaminant, and reaction product particles in a homogeneous aquifer after each step of the EIE sequence given in Table 1. In the first six steps, the west and east wells are operated alternately, first as injection wells (steps 1 and 2) and then as extraction wells (steps 3–6). In the final six steps, the pattern is repeated with the south and north wells. The position and geometry of the plume reflects the rate and location of injection or extraction performed at that step. For instance, the plume is stretched during the injection steps (Figures 3a and 3b), when flow diverges from the active well, and the plume converges toward the active well during the extraction steps (Figures 3c–3f), leading to folding. After the first six steps of the sequence, the plume is folded once; after the final six steps, the plume is folded a second time.

[21] For each step of the EIE sequence, reaction of the contaminant and treatment solution was simulated, as discussed above. Figure 4 (dotted line, circles) presents cumulative percent contaminant mass reacted after each step of the EIE sequence. Particles must be in close proximity to react; for instance, since treatment solution and contaminant particles are initially located adjacent to each other as shown in Figure 1, significant reaction occurs during step 1. EIE reconfigures the arrangement of the particles during each step of the sequence, leading to a measurable amount of reaction in each step. Steps that substantially rearrange the relative particle positions result in more reaction. For example, the plume undergoes significant reconfiguration in step 8, where the plume center is compressed while its extremities are stretched (Figure 3h). This leads to a significant amount of reaction occurring between steps 7 and 8 of the EIE sequence (Figure 4).

[22] EIE was also simulated in a heterogeneous aquifer, represented by the random ln K field shown in Figure 2. Figure 5 illustrates the positions of treatment solution, groundwater contaminant, and reaction product during each step of EIE; the cumulative percent mass reacted is shown in Figure 4 (solid line, circles). The spatially varying ln K of the heterogeneous aquifer produces velocity variations. These velocity variations, combined with the velocity variations that result from the unsteady flow fields generated by EIE, cause more spreading of treatment solution

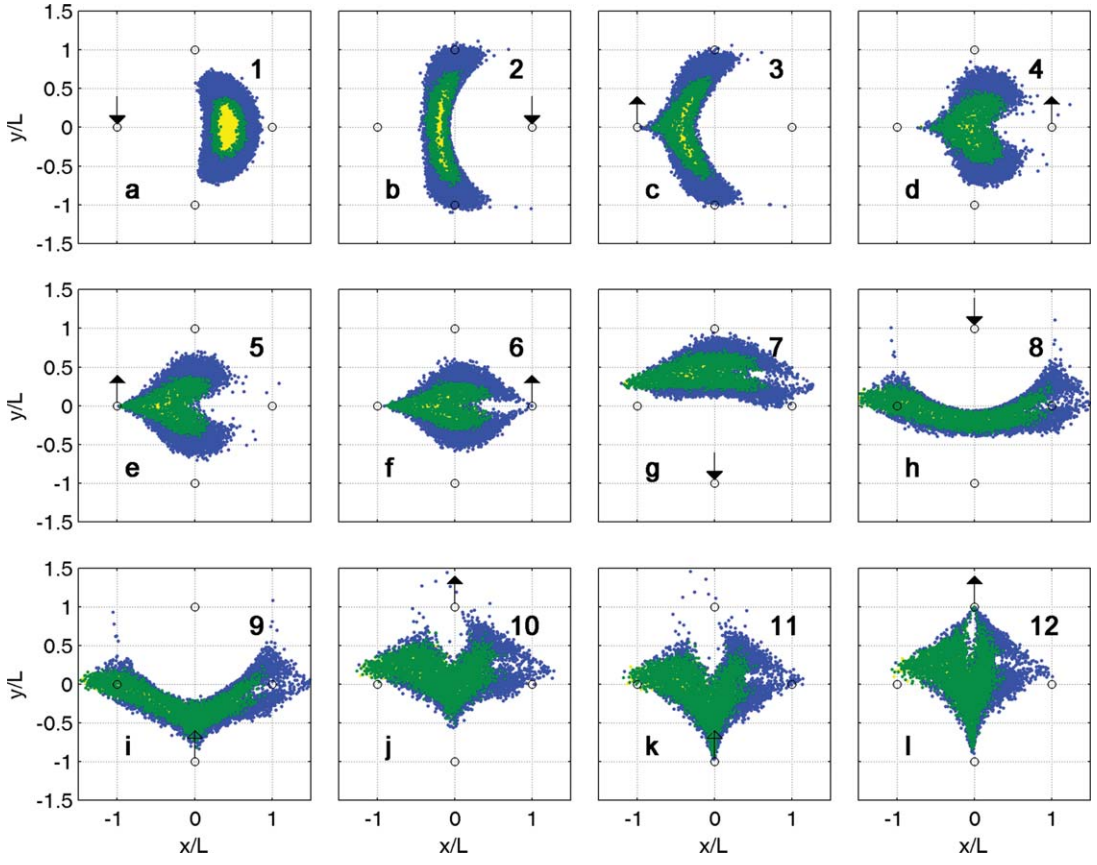

Figure 3. Location of particles of treatment solution (yellow), contaminant (blue), and reaction product (green) during EIE in a homogeneous aquifer. Arrows pointing to small open circles denote the active well for each step of EIE, where arrows pointing down signify injection and arrows pointing up signify extraction. The number in each subplot indicates the step of EIE in Table 1.

and contaminant than in the homogeneous aquifer, and leads to slightly more reaction.

3.2. Reaction Without Engineered Injection and Extraction

[23] To compare the effectiveness of EIE relative to passive in situ remediation, we simulated the movement of the plume in Figure 1 in homogeneous and heterogeneous aquifers without EIE. The final positions of treatment solution, contaminant, and reaction product particles after 75 days (the duration of the EIE sequence in Table 1) are shown in Figures 6a and 6b for the homogeneous and heterogeneous aquifers respectively. The treatment solution and contaminant particles mix somewhat as a result of dispersion; however, the degree of spreading is much lower than with EIE (cf. Figures 6a and 3l and Figures 6b and 5l) for the following reasons. First, because the plume travels with ambient flow only, which provides no folding, particles do not experience dramatic reconfiguration as with EIE. Additionally, since the plume travels at a lower velocity with ambient flow than with EIE, it experiences less spreading due to dispersion, because dispersion is assumed to be proportional to the local velocity, as shown in (4). Note that while the plume experiences more reconfiguration in the heterogeneous aquifer than in the homogeneous aquifer, there is less plume reconfiguration as compared to reconfiguration with EIE (Figure 4). For both aquifers, the amount of contaminant mass reacted is significantly lower without EIE than with EIE. Since spreading is lower as compared to EIE, the amount of reaction by passive spreading during each step is small relative to the amount of reaction by active spreading by EIE. For the homogeneous aquifer, the contaminant mass reacted without EIE is approximately one sixth of mass reacted with EIE, while for the heterogeneous

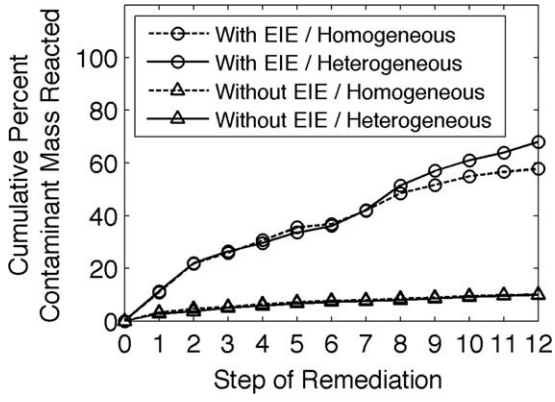

Figure 4. Cumulative percent contaminant mass reacted during in situ remediation.

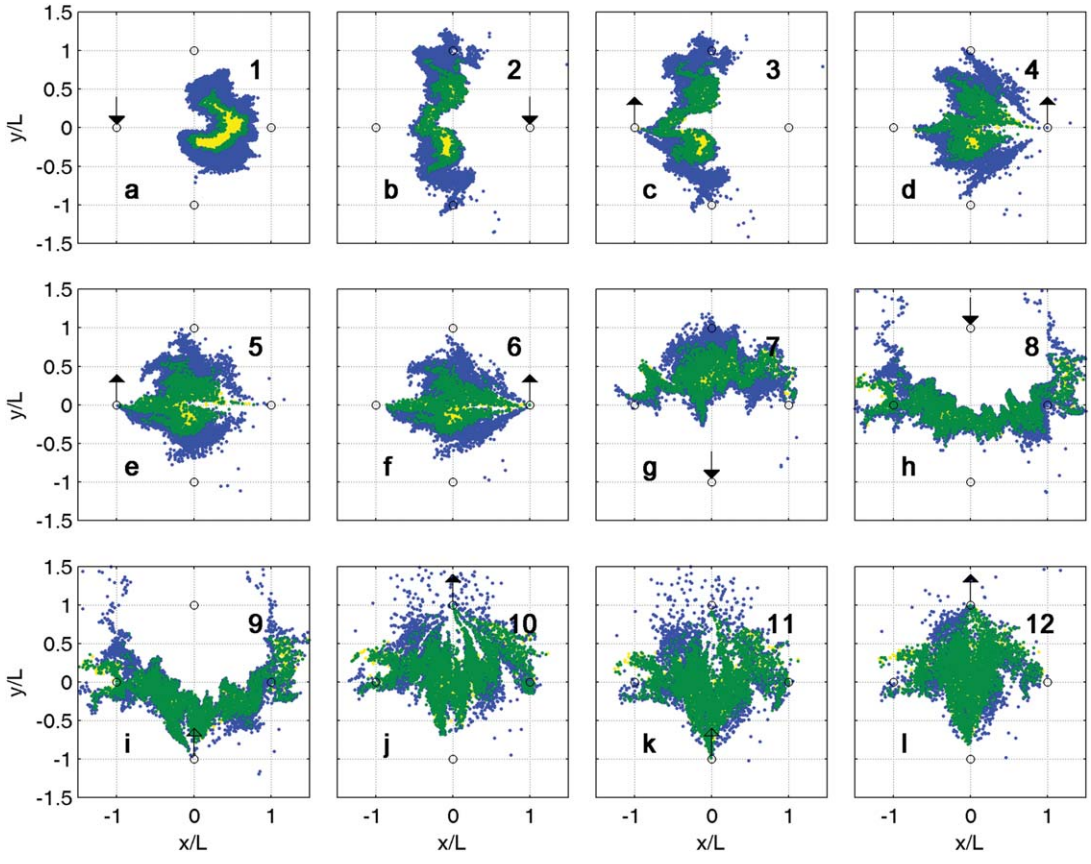

Figure 5. Location of particles of treatment solution (yellow), contaminant (blue), and reaction product (green) during EIE in a heterogeneous aquifer. Arrows pointing to small open circles denote the active well for each step of EIE, where arrows pointing down signify injection and arrows pointing up signify extraction. The number in each subplot indicates the step of EIE.

aquifer, the contaminant mass reacted without EIE is approximately one seventh of the mass reacted with EIE.

3.3. Sensitivity Analysis of Reaction to the Heterogeneity Model

[24] To determine how the amount of reaction depends on the heterogeneity model, we generated 100 realizations each of six different heterogeneous ln K fields using GSLIB by using two different correlation lengths, $\lambda = 0.125L$ (3.125 m) and $\lambda = 0.25L$ (6.25 m), and three different values for the variance of ln K (0.25, 0.5, and 1.0). All ln K fields have a mean K of 0.5 m/d and were generated using a spherical variogram. For each random field, we simulated the movement of the treatment solution, contaminated

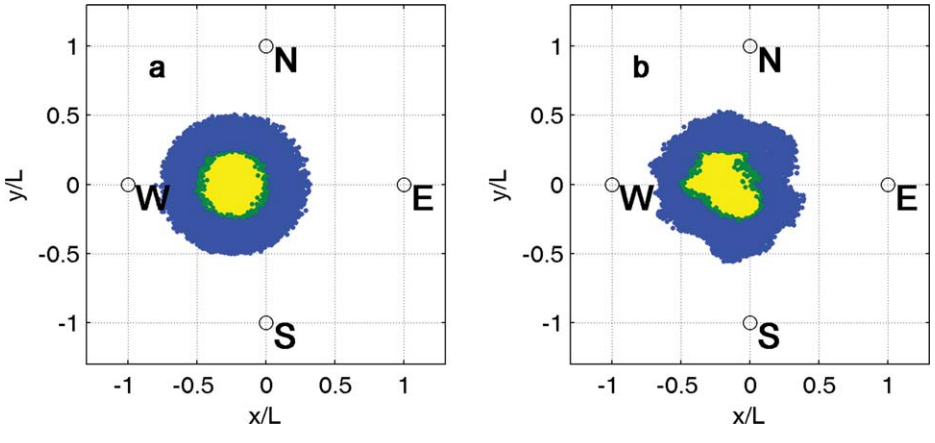

Figure 6. Positions of treatment solution (yellow), contaminant (blue), and reaction product (green) particles after 75 days of travel with ambient groundwater flow in (a) a homogeneous aquifer and (b) a heterogeneous aquifer. Small open circles denote well locations.

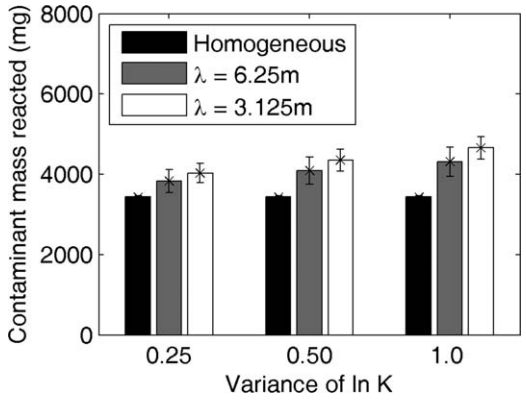

Figure 7. Total contaminant mass reacted during EIE in heterogeneous aquifers with different correlation lengths (λ) for variances of ln K. The error bars represent the standard deviation around the mean total contaminant mass reacted for 100 simulations.

groundwater, and reaction product using the EIE protocol shown in Table 1. Figure 7 shows the average amount of reaction over the 100 realizations of each heterogeneous field after the final step of EIE, with error bars to indicate the standard deviation from the mean. For comparison, the reaction for EIE in a homogeneous aquifer is also shown. In all cases, the amount of reaction in the homogeneous aquifer is less than the amount of reaction in any of the heterogeneous aquifers.

[25] For a fixed correlation length, the average mass reacted increases as the variance of ln K increases. As the variance of ln K increases, the degree of heterogeneity increases; thus local velocity variations also increase, which leads to more spreading of the contaminant and treatment solution plumes, and ultimately more reaction. Also for a fixed correlation length, the standard deviation of the mass reacted increases as the variance of ln K increases.

[26] For a given variance of ln K, the average mass reacted increases as the correlation length decreases (Figure 7). Correlation length determines the proportion of the heterogeneity that the plumes sample during EIE. The plumes move between the four wells, spanning approximately $2L$ (50 m) in the x- and y-directions. With $\lambda = 0.25L$ (6.125 m), the plumes sample approximately 8 correlation lengths in the x- and y-directions; while with $\lambda = 0.125L$ (3.125 m), they sample 16 correlation lengths. Accordingly, as λ decreases, the plumes sample a wider range of hydraulic conductivity, and therefore experience more velocity variations, which generates more spreading, mixing, and reaction. Note that for sufficiently small correlation lengths, the high degree of spreading will lead to a significant amount of the particles being removed at the extraction wells, reducing the amount of reaction that can occur within the aquifer.

[27] Figure 7 also shows that for a given variance of ln K, the standard deviation of the mass reacted over the 100 realizations decreases as the correlation length decreases. In the EIE system, the bulk movement of water is either radially outward from an injection well, or radially inward toward an extraction well; however, heterogeneity causes advective flow paths to deviate from this bulk movement. A random field with a large correlation length contains relatively large isolated regions of low conductivity and of high conductivity; thus the advective flow paths take relatively large excursions from the bulk movement. Since each realization of the random ln K fields has a different pattern of regions with low and high conductivity, the excursions from the bulk movement in each realization occur at different locations, directions, and lengths. Thus, the variability in the shapes of the plumes and in the amount of reaction between realizations is large.

[28] On the other hand, in a random field with a small correlation length, the advective flow paths take relatively small excursions from the bulk movement. Although each realization still leads to a unique plume shape, the variability in the shapes of the plumes and in the amount of reaction is smaller because the excursions are smaller.

[29] Figure 7 also shows that for a given correlation length, the standard deviation of the mass reacted over the 100 realizations increases as the variance of ln K increases. The larger variance of ln K leads to larger excursions from the bulk movement of water, and therefore to more variability in the plume shapes and in the amount of reaction.

4. Discussion

[30] The simulations presented above provide context in which to evaluate the relative effects of passive spreading by heterogeneity versus active spreading by EIE. The benefit of EIE results largely from stretching and folding, which is associated with optimal spreading in laminar flows [*Ottino et al*., 1994]. *Mays and Neupauer* [2012] showed that the EIE sequence used here exhibits chaotic advection and leads to stretching and folding. This stretching and folding results in a significant increase in the length of the perimeter of the treatment solution plume, across which the concentration gradient, ∇C, is large. Regions where the concentration gradient is large are also characterized by a high degree of mixing, as quantified by the local mixing factor, $\nabla^T C \mathbf{D} \nabla C$ [*Dentz et al*., 2011]. Thus, stretching and folding enhances mixing by increasing the area of the aquifer where the local mixing factor is high. Our results show that this ultimately leads to an increase in the mass of contaminant reacted, the ultimate goal of in situ remediation.

[31] Related work by others has shown that the effects of spreading and mixing are distinct at early time, but become effectively linked at later time [*Lester et al*., 2010; *Jha et al*., 2011]. The benefit of EIE would therefore most likely occur at early times, when the structure provided by spreading continues to be relevant, consistent with the work of *Swanson and Ottino* [1990], who emphasized the crucial role of early time behavior when developing applications of chaotic advection.

[32] Our results show that EIE leads to enhanced mixing in a two-dimensional system; however, natural systems are inherently three-dimensional. *Bellin et al.* [2011] noted that pore-scale dispersion is more effective at creating mixing in three-dimensional flows than two-dimensional flows. Thus, our two-dimensional model underestimates the amount of mixing, and also reaction, that would occur in a three-dimensional system. Furthermore, in three-dimensional systems, hydraulic conductivity is typically anisotropic, with longer correlation lengths in the horizontal directions than

in the vertical direction, and this anisotropy enhances mixing as a result of increased disorder of the concentration distribution [*Bellin et al*., 2011]. Hence, in a field application of EIE, we would expect to see more spreading, and therefore more reaction, than is predicted by our two-dimensional model.

[33] The work presented here focuses on nonsorbing solutes that react instantaneously to produce inert reaction products. Investigation of EIE for kinetic reactions and sorbing solutes is the subject of ongoing work. We have not considered reactions whose products could alter the flow field, such as precipitation reactions [*Tartakovsky et al*., 2008] or the growth of microbial biofilms that may lead to clogging [*Li et al*., 2010]. These reactions would lead to more velocity variations, both in ambient flow conditions and with the EIE flow fields; thus we expect that EIE would still lead to enhanced spreading and contaminant degradation.

5. Conclusion

[34] Spreading of a treatment solution into contaminated groundwater results from spatially varying velocity fields, which can be accomplished passively via the heterogeneity of hydraulic conductivity, or actively by injections and extractions chosen to create stretching and folding. *Mays and Neupauer* [2012] proposed engineered injection and extraction, which uses sequential operation of multiple wells, to create stretching and folding to enhance spreading in aquifers. In this study, we demonstrate that in situ remediation with EIE has the potential to significantly increase the amount of reaction as compared to in situ remediation without EIE. In addition we have shown that while heterogeneity promotes spreading and therefore enhances reaction, the amount of spreading and reaction resulting from EIE exceeds the amount of spreading and reaction caused by heterogeneity alone. Finally, we observed that the degree of aquifer heterogeneity impacts the amount of reaction; therefore, the amount of reaction with or without EIE varies depending on the hydraulic properties of the aquifer.

[35] **Acknowledgments.** This work was supported by grants EAR-1113996 and EAR-1114060 from the National Science Foundation. We thank the three anonymous reviewers for valuable comments.

References

Aref, H. (1984), Stirring by chaotic advection, *J. Fluid Mech.*, *143*, 1–21.

Aref, H. (2002), The development of chaotic advection, *Phys. Fluids*, *14*(4), 1315–1325.

Bagtzoglou, A. C., and P. M. Oates (2007), Chaotic advection and enhanced groundwater remediation, *J. Mater. Civil Eng.*, *19*(1), 75–83.

Bellin, A., G. Severino, and A. Fiori (2011), On the local concentration probability density function of solutes reacting upon mixing, *Water Resour. Res.*, *47*, W01514, doi:10.1029/2010WR009696.

Castro-Alcala, E., D. Fernàndez-Garcia, J. Carrera, and D. Bolster (2012), Visualization of mixing processes in a heterogeneous sand box aquifer, *Environ. Sci. Technol.*, *46*, 3228–3235.

Cirpka, O. A. (2005), Effects of sorption on transverse mixing in transient flows, *J. Contam. Hydrol.*, *78*(3), 207–229.

Dagan, G. (1989), *Flow and Transport in Porous Formations*, Springer, Berlin.

Dentz, M., T. Le Borgne, A. Englert, and B. Bijeljic (2011), Mixing, spreading and reaction in heterogeneous media: A brief review, *J. Contam. Hydrol.*, *120-21*, 1–17.

Deutsch, C. and A. Journel (1992), *GSLIB: Geostatistical Software Library and User's Guide*, Oxford Univ. Press, New York.

Harbaugh, A. W., E. R. Banta, M. C. Hill, and M. G. McDonald (2000), MODFLOW-2000, the U.S. Geological Survey modular ground-water model—User guide to modularization concepts and the ground-water flow process, Open-File Rep. 00–92, U.S. Geol. Surv., Reston, Va.

Jha, B., L. Cueto-Felgueroso, and R. Juanes (2011), Fluid mixing from viscous fingering, *Phys. Rev. Lett.*, *106*, 194502, doi:10.1103/PhysRevLett.106.194502.

Kitanidis, P. K. (1994), The concept of the dilution index, *Water Resour. Res.*, *30*(7), 2011–2026.

Le Borgne, T., M. Dentz, D. Bolster, J. Carrera, J. R. de Dreuzy, and P. Davy (2010), Non-Fickian mixing: Temporal evolution of the scalar dissipation rate in heterogeneous porous media, *Adv. Water Resour.*, *33*(12), 1468–1475.

Lester, D. R., M. Rudman, G. Metcalfe, M. G. Trefry, A. Ord, and B. Hobbs (2010), Scalar dispersion in a periodically reoriented potential flow: Acceleration via Lagrangian chaos, *Phys. Rev. E*, *81*, 046319, doi:10.1103/PhysRevE.81.046319.

Li, L., C. I. Steefel, M. B. Kowalsky, A. Englert, and S. S. Hubbard (2010), Effects of physical and geochemical heterogeneities on mineral transformation and biomass accumulation during biostimulation experiments at Rifle, Colorado, *J. Contam. Hydrol.*, *112*(1-4), 45–63.

MacDonald, T. R., and P. K. Kitanidis (1993), Modeling the free-surface of an unconfined aquifer near a recirculation well, *Ground Water*, *31*(5), 774–780.

MacDonald, T. R., P. K. Kitanidis, P. L. McCarty, and P. V. Roberts (1999), Mass-transfer limitations for macroscale bioremediation modeling and implications on aquifer clogging, *Ground Water*, *37*(4), 523–531.

Mays, D. C., and R. M. Neupauer (2012), Plume spreading in groundwater by stretching and folding, *Water Resour. Res.*, *48*, W07501, doi:10.1029/2011WR011567.

Ottino, J. M. (1989), *The Kinematics of Mixing: Stretching*, Chaos, and Transport, Cambridge Univ. Press, Cambridge, U. K.

Ottino, J. M., S. C. Jana, and V. S. Chakravarthy (1994), From Reynolds stretching and folding to mixing studies using horseshoe maps, *Phys. Fluids*, *6*(2), 685–699.

Pollock, D.W. (1994), User's guide for MODPATH/MODPATH-PLOT, version 3: A particle tracking post-processing package for MODFLOW, the U.S. geological survey finite-difference ground-water flow model, Open-File Rep. 94–464, U.S. Geol. Surv., Reston, Va.

Rolle, M., C. Eberhardt, G. Chiogna, O. A. Cirpka, and P. Grathwohl (2009), Enhancement of dilution and transverse reactive mixing in porous media: Experiments and model-based interpretation, *J. Contam. Hydrol.*, *110*(3-4), 130–142.

Sposito, G. (2006), Chaotic solute advection by unsteady groundwater flow, *Water Resour. Res.*, *42*, W06D03, doi:10.1029/2005WR004518.

Swanson, P. D., and J. M. Ottino (1990), A comparative computational and experimental-study of chaotic mixing of viscous fluids, *J. Fluid Mech.*, *213*, 227–249.

Tartakovsky, A. M., G. Redden, P. C. Lichtner, T. D. Scheibe, and P. Meakin (2008), Mixing-induced precipitation: Experimental study and multiscale numerical analysis, *Water Resour. Res.*, *44*, W06S04, doi:10.1029/2006WR005725.

Trefry, M., D. Lester, G. Metcalfe, A. Ord, and K. Regenauer-Lieb (2012), Toward enhanced subsurface intervention methods using chaotic advection, *J. Contam. Hydrol.*, *127*(1-4), 15–29.

Uffink, G. J. M. (1989), Application of Kolmogorov's backward equation in random walk simulations of groundwater contaminant transport, in *Contaminant Transport in Groundwater*, edited by H. E. Kobus and W. Kinzelbach, pp. 283–289, A. A. Balkema, Brookfield, Vermont.

U.S. Environmental Protection Agency. Office of Solid Waste and Emergency Response (1998), *Field Applications of In Situ Remediation Technologies: Chemical Oxidation*. Govern. Print. Off., Washington, D. C.

Wartenburg, D., D. Reyner, and C.S. Scott (2000), Trichloroethylene and cancer: epidemiological evidence. *Environ. Health Perspect. 108*, 161–176.

Weeks, S. W., and G. Sposito (1998), Mixing and stretching efficiency in steady and unsteady groundwater flows, *Water Resour. Res.*, *34*(12), 3315–3322.

Yan, Y. E., and F. W. Schwartz (1999), Oxidative degradation and kinetics of chlorinated ethylenes by potassium permanganate, *J. Contam. Hydrol.*, *37*, 343–365.